On Sparse Grid Interpolation for American Option Pricing with Multiple Underlying Assets

Jiefei Yang[1] and Guanglian Li[1*†]

[1*]Department of Mathematics, The University of Hong Kong, Pokfulam Road, Hong Kong SAR, China.

*Corresponding author(s). E-mail(s): lotusli@maths.hku.hk;
Contributing authors: jiefeiy@connect.hku.hk;
†These authors contributed equally to this work.

Abstract

In this work, we develop a novel efficient quadrature and sparse grid based polynomial interpolation method to price American options with multiple underlying assets. The approach is based on first formulating the pricing of American options using dynamic programming, and then employing static sparse grids to interpolate the continuation value function at each time step. To achieve high efficiency, we first transform the domain from $\mathbb{R}^{\boldsymbol{d}}$ to $\boldsymbol{(-1,1)^d}$ via a scaled tanh map, and then remove the boundary singularity of the resulting multivariate function over $\boldsymbol{(-1,1)^d}$ by a bubble function and simultaneously, to significantly reduce the number of interpolation points. We rigorously establish that with a proper choice of the bubble function, the resulting function has bounded mixed derivatives up to a certain order, which provides theoretical underpinnings for the use of sparse grids. Numerical experiments for American arithmetic and geometric basket put options with the number of underlying assets up to 16 are presented to validate the effectiveness of our approach.

Keywords: sparse grids, American option pricing, multiple underlying assets, continuation value function, quadrature

MSC Classification: 65D40 , 91G20

1 Introduction

This paper is concerned with American option pricing with payoffs affected by many underlying instruments, which can be assets such as stocks, bonds, currencies, commodities, and indices (e.g., S&P 500, NASDAQ 100) [1, p. 365]. Classical examples include pricing American max-call and basket options [2–8]. In practice, American options can be exercised only at discrete dates. The options that can be exercised only at finite discrete dates are called Bermudan options, named after the geographical feature of Bermudan Islands (i.e., being located between America and Europe while much closer to the American seashore) [9]. Merton [10] showed that pricing an American call option on a single asset with no dividend is equivalent to pricing a European option, and obtained an explicit solution to pricing perpetual American put. However, except these two cases no closed-form solution is known to price American options even in the simplest Black Scholes model. Thus it is imperative to develop efficient numerical methods for American option pricing.

Various numerical methods have been proposed for pricing and hedging in the past five decades, using different formulations of American option pricing, e.g., an optimal stopping problem, a variational inequality, or a free boundary problem [11–14]. A finite difference method (FDM) was proposed to price American options based on variational inequalities [15], with its convergence proved in [12] by showing that the $\mathcal{C}^1$ regularity of the value function with respect to the underlying price. The binomial options pricing model (BOPM) based upon optimal time stopping was developed in [16], and its convergence was shown in [17]. When the number d of underlying assets is smaller than four, one can extend one-dimensional pricing methods using tensor product or additional treatment to price multi-asset options. For example, Cox-Ross-Rubinstein (CRR) binomial tree model can be extended to the multinomial option pricing model to price American options with two underlying assets [18]. However, dynamic programming (cf. (3) below) or variational inequalities [19] are predominant when d is greater than three. Many numerical schemes have been developed based on the variational inequalities, e.g., FDMs [15, 20, 21] and finite element methods (FEMs) [5]. However, only the first order convergence rate can be achieved, since the value function has only $\mathcal{C}^1$ regularity with respect to the underlying price (i.e., smooth pasting condition [22]).

There are mainly two lines of research on American option pricing based on dynamic programming, i.e., simulation based methods [2, 23, 24] and quadrature and interpolation (Q&I) based methods [25, 26]. Simulation based methods are fast and easy to implement, but their accuracy is hard to justify. One representative method is the least square Monte Carlo method [23], which employs least square regression and Monte Carlo method to approximate conditional expectations, cf. (3). Q&I based methods employ quadrature to approximate conditional expectations and interpolation to construct function approximators. One can use Gaussian quadrature or adaptive quadrature to approximate conditional expectations in (3) and Chebyshev polynomial interpolation, spline interpolation or radial basis functions to reconstruct the continuation value or the value function [25, 26]. In [27], a dynamic Chebyshev method via polynomial interpolation of the value functions was developed, allowing the generalized moments evaluation in the offline stage to reduce computational

complexity. Although Q&I based methods are efficient in low-dimensional settings, the extensions to high-dimensional cases are highly nontrivial, and there are several outstanding challenges, e.g., curse of dimensionality, unboundedness of the domain and the absence of natural boundary conditions. For example, if the domain is truncated and artificial boundary conditions are imposed, then one is actually pricing an American barrier option with rebate instead of the American option itself. Accurate boundary conditions can be obtained by pricing a $(d-1)$-dimensional problem [6], which, however, is still computationally challenging.

The sparse grids technique has been widely used in option pricing with multiple underlying assets, due to its capability to approximate high-dimensional functions with bounded mixed derivatives, for which the computational complexity for a given accuracy does not grow exponentially with respect to d [28]. It has been applied to price multi-asset European and path-dependent Asian options, by formulating them as a high-dimensional integration problem [29–31], and also combined with the FDMs [7] and FEMs [32] to price options with $d \leq 5$. In the context of Q&I methods, adaptive sparse grids interpolation with local linear hierarchical basis have been used to approximate value functions [8].

In this work, we propose a novel numerical approach to price American options under multiple underlying assets, which is summarized in Algorithm 1. It crucially draws on the $\mathcal{C}^\infty$ regularity of the continuation value function, cf. (4), and uses sparse grid Chebyshev polynomial interpolation to alleviate the curse of dimensionality. This is achieved in several crucial steps. First, we transform the unbounded domain $\mathbb{R}^d$ into a bounded one, which eliminates the need of imposing artificial boundary conditions. Second, to further improve the computational efficiency, using a suitable bubble function, we obtain a function that can be continuously extended to the boundary with vanishing boundary values and with bounded mixed derivatives up to certain orders, which is rigorously justified in Theorem 1. This construction enables the use of the standard sparse grid technique with much fewer sparse grids (without adaptivity), and moreover, the interpolation functions fulfill the requisite regularity conditions, thereby admitting theoretical convergence guarantees. The distinct features of the proposed method include using static sparse grids at all time steps and allowing deriving the value function on the whole domain $\mathbb{R}^d$, and thus can also be used to estimate important parameters, e.g., hedge ratio.

Extensive numerical experiments demonstrate that Algorithm 1 can break the curse of dimensionality in the sense that high accuracy is achieved with involved computational complexity being almost independent of the dimension. We show both numerically and theoretically the robustness of Algorithm 1, and numerically we observe that this algorithm can be combined with any kind of quadrature schemes. Up to our best knowledge, there is no accurate reference solutions for American arithmetic basket put options beyond six underlying assets. Consequently, our numerical results up to $d = 12$ in this case make more accurate reference solutions available and thus can promote the research on higher dimensions substantially. To demonstrate the accuracy of our algorithm, we calcuate the price of American geometric basket put options up to $d = 16$. In both cases, we consistently observe high accuracy

of Algorithm 1, with almost no influence from the dimension. To sum up, our proposed algorithm significantly improves over the state-of-the-art pricing schemes for American options with multiple underlying assets and in the meanwhile has rigorous theoretical guarantee.

The remainder of our paper is structured as follows. In Section 2, we derive the continuation value function $f_k(\mathbf{x})$ for an American basket put option with underlying assets following the correlated geometric Brownian motion under the risk-neutral probability. In Section 3, we develop the novel method. In Section 4, we establish the smoothness of the interpolation function in the space of functions with bounded mixed derivatives. In Section 5, we present extensive numerical tests for American basket options with up to 16 underlying assets. Finally, we conclude with future work in Section 6.

2 The mathematical model

Martinagle pricing theory gives the fair price of an American option as the solution to the optimal stopping problem in the risk-neutral probability space $(\Omega, \mathcal{F}, (\mathcal{F}_t)_{0\le t\le T}, \mathbb{Q})$:

$$V(t) = \sup_{\tau_t\in[t,T]} \mathbb{E}[e^{-r(\tau_t - t)} g(\mathbf{S}(\tau_t))|\mathcal{F}_t], \tag{1}$$

where τ_t is a $\mathcal{F}_t$-stopping time, T is the expiration date, $(\mathbf{S}(t))_{0\le t\le T}$, is a collection of d-dimensional price processes, and $g(\cdot)$ is the payoff function depending on the type of the option. The payoffs of put and call options take the following form $g(\mathbf{S}) = \max(\kappa - \Psi(\mathbf{S}), 0)$ and $g(\mathbf{S}) = \max(\Psi(\mathbf{S}) - \kappa, 0)$, respectively, where $\Psi : \mathbb{R}^d_+ \to \mathbb{R}_+$, and κ is the strike price.

Now we describe a detailed mathematical model for pricing an American put option on d underlying assets with a strike price κ and a maturity date T, whose numerical approximation is the main objective of this work. One classical high-dimensional example is pricing American basket options. Let $g : \mathbb{R}^d_+ \to \mathbb{R}_+$ be its payoff function, and assume that the prices of the underlying assets $\mathbf{S}(t) = [S^1(t), \dots, S^d(t)]^\top$ follow the correlated geometric Brownian motions

$$\mathrm{d}S^i(t) = (r - \delta_i)S^i(t)\,\mathrm{d}t + \sigma_i S^i(t)\,\mathrm{d}\tilde{W}^i(t) \quad \text{with } S^i(0) = S^i_0, \quad i = 1, 2, \dots, d, \tag{2}$$

where $\tilde{W}^i(t)$ are correlated $\mathbb{Q}$-Brownian motions with $\mathbb{E}[\mathrm{d}\tilde{W}^i(t)\mathrm{d}\tilde{W}^j(t)] = \rho_{ij}\,\mathrm{d}t$, $\rho_{ii} = 1$ for $i, j = 1, 2, \dots, d$, and r, δ_i and σ_i are the riskless interest rate, dividend yields, and volatility parameters, respectively. The payoffs of an arithmetic and a geometric basket put are respectively given by

$$g(\mathbf{S}) = \max\left(\kappa - \frac{1}{d}\sum_{i=1}^{d} S^i, 0\right) \quad \text{and} \quad g(\mathbf{S}) = \max\left(\kappa - \left(\prod_{i=1}^{d} S^i\right)^{1/d}, 0\right).$$

In practice, the $\mathcal{F}_0$-stopping time τ_0 is assumed to be taken in a set of discrete time steps, $\mathcal{T}_{0,T} := \{t_k = k\Delta t : k = 0, 1, \ldots, K\}$, with $\Delta t = T/K$. This leads to the pricing of a K-times exercisable Bermudan option that satisfies the following dynamic programming problem

$$\begin{aligned} &\mathcal{V}_K(\mathbf{s}) = g(\mathbf{s}), \\ &\mathcal{V}_k(\mathbf{s}) = \max\left(g(\mathbf{s}), \mathbb{E}[e^{-r\Delta t}\mathcal{V}_{k+1}(\mathbf{S}_{k+1})|\mathbf{S}_k = \mathbf{s}]\right) \quad \text{for } k \le K-1, \end{aligned} \tag{3}$$

where $\mathcal{V}_k$ is called the value function at time t_k and $\mathbf{S}_k := \mathbf{S}(t_k)$ is the discretized price processes. Throughout, for a stochastic process $\mathbf{X}(t)$, we write $\mathbf{X}_k := \mathbf{X}(t_k)$, $k = 0, 1, \ldots, K$. Note that by the Markov property of Itô process, we can substitute the conditional expectation conditioning on $\mathcal{F}_{t_k}$ to $\mathbf{S}_k$. The conditional expectation as a function of prices is called the continuation value function, i.e.,

$$C_k(\mathbf{s}) = \mathbb{E}[e^{-r\Delta t}\mathcal{V}_{k+1}(\mathbf{S}(t_{k+1}))|\mathbf{S}(t_k) = \mathbf{s}] \text{ for } k = 0, 1, \ldots, K-1. \tag{4}$$

Below we recast problem (3) in terms of the continuation value function

$$\begin{aligned} C_{K-1}(\mathbf{s}) &= \mathbb{E}\left[e^{-r\Delta t}g(\mathbf{S}_K)|\mathbf{S}_{K-1} = \mathbf{s}\right], \\ C_k(\mathbf{s}) &= \mathbb{E}\left[e^{-r\Delta t}\max\left(g(\mathbf{S}_{k+1}), C_{k+1}(\mathbf{S}_{k+1})\right)|\mathbf{S}_k = \mathbf{s}\right] \quad \text{for } k \le K-2. \end{aligned} \tag{5}$$

Given an approximation to $C_0(\mathbf{s})$, the price of Bermudan option can be obtained by

$$\mathcal{V}_0(\mathbf{S}_0) = \max(g(\mathbf{S}_0), C_0(\mathbf{S}_0)). \tag{6}$$

The reformulation in terms of C_k is crucial to the development of the numerical scheme.

Next we introduce the rotated log-price, which has independent components with Gaussian densities. We denote the correlation matrix as $P = (\rho_{ij})_{d\times d}$, the volatility matrix Σ as a diagonal matrix with volatility σ_i on the diagonal, and write the dividend yields as a vector $\boldsymbol{\delta} = [\delta_1, \ldots, \delta_d]^\top$. Then the log-price $\mathbf{X}(t)$ with each component defined by $X^i(t) := \ln(S^i(t)/S_0^i)$ follows a multivariate Gaussian distribution

$$\mathbf{X}(t) \sim \mathcal{N}\left(\left(r - \boldsymbol{\delta} - \frac{1}{2}\Sigma^2\mathbf{1}\right)t, \Sigma P\Sigma^\top t\right),$$

with $\mathbf{1} := [1, 1, \ldots, 1]^\top \in \mathbb{R}^d$. The covariance matrix $\Sigma P\Sigma^\top$ admits the spectral decomposition $\Sigma P\Sigma^\top = Q^\top\Lambda Q$. Then the rotated log-price $\tilde{\mathbf{X}}(t) := Q^\top\mathbf{X}(t)$ follows an independent Gaussian distribution

$$\tilde{\mathbf{X}}(t) \sim \mathcal{N}\left(Q^\top\left(r - \boldsymbol{\delta} - \frac{1}{2}\Sigma^2\mathbf{1}\right)t, \Lambda t\right).$$

Therefore, to eliminate the correlation, we introduce the transformation

$$\tilde{\mathbf{X}}(t) := Q^\top \ln(\mathbf{S}(t)./\mathbf{S}_0),$$

and denote the inverse transformation by

$$\phi(\tilde{\mathbf{X}}(t)) := \mathbf{S}(t) = \mathbf{S}_0 . * \exp(Q\tilde{\mathbf{X}}(t)),$$

where ./ and .∗ represent component-wise division and multiplication.

Finally, by defining $f_k(\mathbf{x}) := C_k(\phi(\mathbf{x}))$ as the continuation value function with respect to the rotated log-price for $\mathbf{x} \in \mathbb{R}^d$, we obtain the following dynamic programming procedure

$$\begin{aligned} f_{K-1}(\mathbf{x}) &= \mathbb{E}\left[e^{-r\Delta t} g(\phi(\tilde{\mathbf{X}}_K)) \middle| \tilde{\mathbf{X}}_{K-1} = \mathbf{x}\right], \\ f_k(\mathbf{x}) &= \mathbb{E}\left[e^{-r\Delta t} \max\left(g(\phi(\tilde{\mathbf{X}}_{k+1})), f_{k+1}(\tilde{\mathbf{X}}_{k+1})\right) \middle| \tilde{\mathbf{X}}_k = \mathbf{x}\right] \text{ for } k \le K-2. \end{aligned} \tag{7}$$

The main objective of this work is to develop an efficient numerical method for solving problem (7) with a large number of dimension d. The detailed construction is given in Section 3.

3 Methodologies

In this section, we systematically develop a novel algorithm, based on quadrature and sparse grids polynomial interpolation (SGPI) [33] to solve problem (7) so that highly accurate results can be obtained for moderately large dimensions. This is achieved as follows. First, we propose a mapping ψ (8) that transforms the domain from $\mathbb{R}^d$ to $\Omega := (-1, 1)^d$, and obtain problem (10) with the unknown function F_k defined over the hypercube Ω in Section 3.1. The mapping ψ enables utilizing identical sparse grids for all time stepping $k = K-1 : -1 : 0$, which greatly facilitates the computation, and moreover, it avoids domain truncation and artificial boundary data when applying SGPI, which eliminates extra approximation errors. However, the partial derivatives of F_k may have boundary singularities, leading to low-efficiency of SGPI. To resolve this issue, we multiply F_k with a bubble function (11), and derive problem (12) with unknown functions u_k defined over the hypercube Ω. Second, we present the SGPI of the unknown u_k in Section 3.2. Third and last, we provide several candidates for quadrature rules and summarize the algorithm in Section 3.3, and analyze its complexity.

3.1 Mapping for unbounded domains and bubble functions

A direct application of the SGPI to problem (7) is generally involved since the problem is formulated on $\mathbb{R}^d$. For $d = 1$, quadrature and interpolation-based schemes can be applied to problem (7) with domain truncation and suitable boundary conditions, e.g., payoff function. However, for $d \ge 2$, the exact boundary conditions of the truncated domain requires solving $(d-1)$-dimensional American option pricing problems [6]. Therefore, the unboundedness of the domain $\mathbb{R}^d$ and the absence of natural boundary conditions pose great challenges to develop direct yet efficient interpolation for the continuation value function f_k, and there is an imperative need to develop a new approach to overcome these challenges.

Inspired by spectral methods on unbounded domains [34], we propose the use of the logarithmic transformation $\psi : \mathbb{R}^d \to \Omega := (-1,1)^d$, defined by

$$\begin{cases} \mathbf{Z} = \psi(\tilde{\mathbf{X}}) \text{ with each component } Z^i := \tanh(L\tilde{X}^i) \in (-1,1), \\ \tilde{\mathbf{X}} = \psi^{-1}(\mathbf{Z}) \text{ with each component } \tilde{X}^i := L^{-1}\operatorname{arctanh}(Z^i) \in \mathbb{R}, \end{cases} \tag{8}$$

where $L > 0$ is a scale parameter controlling the slope of the mapping. The logarithmic mapping ψ is employed since the transformed points decay exponentially as they tend to infinity. Asymptotically the exponential decay rate matches that of the Gaussian distribution of the rotated log-price $\tilde{\mathbf{X}}(t)$. Then by Itô's lemma, the new stochastic process $\mathbf{Z}(t) = [Z^1(t), \ldots, Z^d(t)]^\top$ satisfies the stochastic differential equations

$$\mathrm{d}Z^i(t) = L\left(1 - (Z^i(t))^2\right)\left((\mu_i - \lambda_i L Z^i(t))\,\mathrm{d}t + \sqrt{\lambda_i}\,\mathrm{d}W^i(t)\right) \text{ for } i = 1, \ldots, d, \tag{9}$$

where $\boldsymbol{\mu} = [\mu_1, \ldots, \mu_d]^\top = Q^\top\left(r - \boldsymbol{\delta} - \frac{1}{2}\Sigma^2\mathbf{1}\right)$, λ_i are diagonal elements of Λ, and $W^i(t)$ are independent standard Brownian motions. Note that the drift and diffusion terms in (9) vanish on the boundary $\partial\Omega$. Thus, (9) fulfills the reversion condition [35], which implies $\mathbf{Z}(t) \in \Omega$ for $t > s$ provided $\mathbf{Z}(s) \in \Omega$.

Then we apply the mapping ψ to the dynamic programming procedure (7). Let $F_k(\mathbf{z}) := f_k(\psi^{-1}(\mathbf{z})) = C_k\left(\phi(\psi^{-1}(\mathbf{z}))\right)$ be the continuation value function of the bounded variable $\mathbf{z}$. Then problem (7) can be rewritten as, for any $\mathbf{z} \in \Omega$,

$$\begin{aligned} F_{K-1}(\mathbf{z}) &= \mathbb{E}\left[e^{-r\Delta t} g\left(\phi(\psi^{-1}(\mathbf{Z}_K))\right) \middle| \mathbf{Z}_{K-1} = \mathbf{z}\right], \\ F_k(\mathbf{z}) &= \mathbb{E}\left[e^{-r\Delta t} \max\left(g\left(\phi(\psi^{-1}(\mathbf{Z}_{k+1}))\right), F_{k+1}(\mathbf{Z}_{k+1})\right) \middle| \mathbf{Z}_k = \mathbf{z}\right], \; k \le K-2. \end{aligned} \tag{10}$$

Below we denote by $H(\cdot) := g\left(\phi(\psi^{-1}(\cdot))\right)$ the payoff function with respect to the bounded variable $\mathbf{z}$.

Note that problem (10) is posed on the bounded domain $\Omega := (-1,1)^d$, $d \ge 1$, which however remains challenging to approximate. First, the function $F_k : \Omega \to \mathbb{R}$ may have singularities on the boundary $\partial\Omega$ due to the use of the mapping ψ. Second, the Dirichlet boundary condition of F_k is not identically zero, which is undesirable for controlling the computational complexity of the algorithm, especially in high dimensions. Thus, we employ a bubble function of the form

$$b(\mathbf{z}) = \prod_{i=1}^{d}(1 - z_i^2)^\beta, \quad \mathbf{z} \in \overline{\Omega} := [-1,1]^d, \tag{11}$$

where the parameter $\beta > 0$ controls the shape of $b(\mathbf{z})$. Note that $b(\mathbf{z}) > 0$ for $\mathbf{z} \in \Omega$ and $b(\mathbf{z}) = 0$ on $\partial\Omega$. Let

$$u_k(\mathbf{z}) := F_k(\mathbf{z})b(\mathbf{z}), \quad k = 0, \ldots, K-1.$$

Then the dynamic programming problem (10) is equivalent to

$$\begin{aligned} u_{K-1}(\mathbf{z}) &= \mathbb{E}\left[e^{-r\Delta t}H(\mathbf{Z}_K)|\mathbf{Z}_{K-1}=\mathbf{z}\right] b(\mathbf{z}), \\ u_k(\mathbf{z}) &= \mathbb{E}\left[e^{-r\Delta t}\max\left(H(\mathbf{Z}_{k+1}), \frac{u_{k+1}(\mathbf{Z}_{k+1})}{b(\mathbf{Z}_{k+1})}\right)\middle|\mathbf{Z}_k=\mathbf{z}\right] b(\mathbf{z}),\ k \le K-2. \end{aligned} \tag{12}$$

Remark 1 *The term* $\frac{u_{k+1}(\mathbf{Z}_{k+1})}{b(\mathbf{Z}_{k+1})}$ *appearing in* (12) *is well-defined for* $\mathbf{Z}_{k+1} \in \Omega$. *Nevertheless, since the bubble function* $b(\mathbf{z})$ *approaches zero as* $\mathbf{z} \to \partial\Omega$, *in the numerical experiments, one should guarantee that* $b(\cdot)$ *evaluated on the computational grid will be greater than the machine epsilon, e.g.,* $\varepsilon = 2.2204 \times 10^{-16}$ *in MATLAB. This will be established in Proposition 1.*

3.2 Approximation by sparse grids polynomial interpolation (SGPI)

Next, we apply SGPI [33] to approximate the zero extension $\overline{u}_k : \overline{\Omega} \to \mathbb{R}$ of u_k iteratively backward in time. By choosing suitable bubble functions $b(\mathbf{z})$, we shall prove in Theorem 1 below the smoothness property of $\overline{u}_k$ up to order r. Thus SGPI achieves a geometrical convergence rate with respect to the number of interpolation points $\tilde{N}$, which depends only on the dimension d in a logarithm term, i.e. $\mathcal{O}(\tilde{N}^{-r}(\log \tilde{N})^{(r+1)(d-1)})$ as stated in Proposition 2. Moreover, since $\overline{u}_k$ vanishes over the boundary, then the required number of interpolation data is greatly reduced.

SGPI [33] (also called Smolyak approximation) is a powerful tool for constructing function approximations over a high-dimensional hypercube. Consider a function $f : \overline{\Omega} \to \mathbb{R}$. For $d = 1$, we denote by $X^\ell = \{x_1^\ell, \ldots, x_{N_\ell}^\ell\}$ the set of nested Chebyshev-Gauss-Lobatto (CGL) points, with the nodes x_j^ℓ given by

$$x_j^\ell = \begin{cases} 0 & \text{for } j = 1 \text{ if } \ell = 1, \\ \cos(\frac{(j-1)\pi}{N_\ell - 1}) & \text{for } j = 1, \ldots, N_\ell \text{ if } \ell \ge 2. \end{cases}$$

The cardinality of the set X^ℓ is

$$N_\ell = \begin{cases} 1 & \text{if } \ell = 1, \\ 2^{\ell-1} + 1 & \text{if } \ell \ge 2. \end{cases}$$

The polynomial interpolation $U^\ell f$ of f over the set X^ℓ is defined as follows. For $\ell = 1$, consider the midpoint rule, i.e., $(U^1 f)(x) = f(0)$. For $\ell \ge 2$, $U^\ell f$ is given by

$$(U^\ell f)(x) = \sum_{j=1}^{N_\ell} f(x_j^\ell) L_j^\ell(x), \quad \text{with } L_j^\ell(x) = \prod_{k=1, k\neq j}^{N_\ell} \frac{x - x_k}{x_j - x_k},$$

where L_j^ℓ are Lagrange basis polynomials. Then we define the difference operator

$$\Delta^\ell f = (U^\ell - U^{\ell-1})f \quad \text{with } U^0 f = 0.$$

For $d > 1$, Smolyak's formula approximates a function $f : \overline{\Omega} \to \mathbb{R}$ by the interpolation operator

$$A(q,d) = \sum_{\boldsymbol{\ell} \in I(q,d)} \Delta^{\ell_1} \otimes \cdots \otimes \Delta^{\ell_d},$$

with the index set $I(q,d) := \{\boldsymbol{\ell} \in \mathbb{N}^d : |\boldsymbol{\ell}| \le q\}$ and $|\boldsymbol{\ell}| = \ell_1 + \cdots + \ell_d$ [33]. Equivalently, the linear operator $A(q,d)$ can be represented as [36, Lemma 1]

$$A(q,d) = \sum_{\boldsymbol{\ell} \in P(q,d)} (-1)^{q-|\boldsymbol{\ell}|} \binom{d-1}{q-|\boldsymbol{\ell}|} U^{\ell_1} \otimes \cdots \otimes U^{\ell_d}, \tag{13}$$

with the index set $P(q,d) := \{\boldsymbol{\ell} \in \mathbb{N}^d : q - d + 1 \le |\boldsymbol{\ell}| \le q\}$, where the tensor product of the univariate interpolation operators is defined by

$$(U^{\ell_1} \otimes \cdots \otimes U^{\ell_d})(f) = \sum_{j_1=1}^{N_{\ell_1}} \cdots \sum_{j_d=1}^{N_{\ell_d}} f(x_{j_1}^{\ell_1}, \ldots, x_{j_d}^{\ell_d})(L_{j_1}^{\ell_1} \otimes \cdots \otimes L_{j_d}^{\ell_d}),$$

i.e., multivariate Lagrange interpolation. With the set X^{ℓ_i} (i.e., one-dimensional nested CGL points), the formula (13) indicates that computing $A(q,d)(f)$ only requires function evaluations on the sparse grids

$$H(q,d) = \bigcup_{\boldsymbol{\ell} \in P(q,d)} X^{\ell_1} \times \cdots \times X^{\ell_d}.$$

We denote the cardinality of $H(q,d)$ by $\tilde{N}_{CGL}(q,d)$. Usually, the interpolation level $L_I \in \mathbb{N}_0$ is defined by

$$L_I := q - d.$$

Then for fixed L_I and $d \to \infty$, the following asymptotic estimate of $\tilde{N}_{CGL}(L_I + d, d)$ holds [37]

$$\tilde{N}_{CGL}(L_I + d, d) \approx \frac{2^{L_I}}{L_I!} d^{L_I}. \tag{14}$$

The sparse grid has much fewer grid points than the full grid generated by the tensor product. Furthermore, in high-dimensional hypercube, a significant amount of sparse grids lie on the boundary. We will compare the number of CGL sparse grids $\tilde{N}_{CGL}(L_I + d, d)$ and the number of inner sparse grids N in Section 3.3. Note that for all inner sparse grids $\{\mathbf{z}^n\}_{n=1}^N$ of the interpolation level L_I, each coordinate z_j^n satisfies

$$-\cos\left(\frac{\pi}{2^{\ell_j - 1}}\right) \le z_j^n \le \cos\left(\frac{\pi}{2^{\ell_j - 1}}\right), \tag{15}$$

where $\ell_1 + \cdots + \ell_d \le L_I + d$.

3.3 Numerical algorithm

We interpolate the function $\overline{u}_k : \overline{\Omega} \to \mathbb{R}$ on CGL sparse grids in the dynamic programming (12), where the interpolation data can be formulated as high-dimensional integrals. Since $\overline{u}_k(\mathbf{z}) = 0$ for $\mathbf{z} \in \partial\Omega$, only function evaluations on the inner sparse grids are required. This greatly reduces the computational complexity, especially for large d. Indeed, since $\tilde{\mathbf{X}}_{k+1} = \tilde{\mathbf{X}}_k + \mathbf{Y}$ with $\mathbf{Y} \sim \mathcal{N}(Q^\top(r - \boldsymbol{\delta} - \frac{1}{2}\Sigma^2\mathbf{1})\Delta t, \Lambda\Delta t)$,

$$\mathbf{Z}_{k+1} = \psi(\psi^{-1}(\mathbf{Z}_k) + \mathbf{Y}). \tag{16}$$

For a fixed interpolation knot $\mathbf{z} \in \Omega$, we denote

$$v_{k+1}^{\mathbf{z}}(\mathbf{Y}) = \max\left(H\big(\psi(\psi^{-1}(\mathbf{z}) + \mathbf{Y})\big), \frac{u_{k+1}}{b}\big(\psi(\psi^{-1}(\mathbf{z}) + \mathbf{Y})\big)\right), \tag{17}$$

and the probability density of $\mathbf{Y}$ as $\rho(\mathbf{y}) = \prod_{i=1}^d \rho_i(y_i)$. Following (12), the interpolation data $u_k(\mathbf{z})$ is given by

$$u_k(\mathbf{z}) = e^{-r\Delta t}\mathbb{E}[v_{k+1}^{\mathbf{z}}(\mathbf{Y})]b(\mathbf{z}) = e^{-r\Delta t}b(\mathbf{z})\int_{\mathbb{R}^d} v_{k+1}^{\mathbf{z}}(\mathbf{y})\rho(\mathbf{y})\,\mathrm{d}\mathbf{y},$$

where the last integral can be computed by any high-dimensional quadrature methods, e.g., Monte Carlo (MC), quasi-Monte Carlo (QMC) method, or sparse grid quadrature.

1. The **Monte Carlo method** approximates the integral by averaging random samples of the integrand

$$\int_{\mathbb{R}^d} v_{k+1}^{\mathbf{z}}(\mathbf{y})\rho(\mathbf{y})\,\mathrm{d}\mathbf{y} \approx \frac{1}{M}\sum_{m=1}^M v_{k+1}^{\mathbf{z}}(\mathbf{y}^m), \tag{18}$$

   where $\{\mathbf{y}^m\}_{m=1}^M$ are independent and identically distributed (i.i.d.) random samples drawn from the distribution $\rho(\mathbf{y})$.
2. The **Quasi-Monte Carlo method** takes the same form as (18), but $\{\mathbf{y}^m\}_{m=1}^M$ are the transformation of QMC points. By changing variables $\mathbf{x} = \Phi(\mathbf{y})$ with Φ being the cumulative density function (CDF) of $\mathbf{Y}$, we have

$$\begin{aligned}\int_{\mathbb{R}^d} v_{k+1}^{\mathbf{z}}(\mathbf{y})\rho(\mathbf{y})\,\mathrm{d}\mathbf{y} &= \int_{[0,1]^d} v_{k+1}^{\mathbf{z}}\left(\Phi^{-1}(\mathbf{x})\right)\,\mathrm{d}\mathbf{x} \\ &\approx \frac{1}{M}\sum_{m=1}^M v_{k+1}^{\mathbf{z}}\left(\Phi^{-1}(\mathbf{x}^m)\right) = \frac{1}{M}\sum_{m=1}^M v_{k+1}^{\mathbf{z}}(\mathbf{y}^m),\end{aligned} \tag{19}$$

   where $\{\mathbf{x}^m\}_{m=1}^M$ are QMC points taken from a low-discrepancy sequence, e.g., Sobol sequence and sequences generated by the lattice rule. Note that other transformations Φ are also available for designing QMC approximation [38].
3. The **Sparse grid quadrature** approximates the integral based on a combination of tensor products of univariate quadrature rule. For the integration with Gaussian

measure, several types of sparse grids are available, including Gauss-Hermite, Genz-Keister, and weighted Leja points [39]. Let $(\omega_m, \mathbf{y}^m)_{m=1}^M$ be quadrature weights and points associated with an anisotropic Gaussian distribution of $\mathbf{Y}$. Then the integral is computed by

$$\int_{\mathbb{R}^d} v_{k+1}^{\mathbf{z}}(\mathbf{y})\rho(\mathbf{y})\,\mathrm{d}\mathbf{y} \approx \sum_{m=1}^{M} \omega_m v_{k+1}^{\mathbf{z}}(\mathbf{y}^m). \tag{20}$$

By employing the transformation between the asset price $\mathbf{S}$ and the bounded variable $\mathbf{z}$, the sparse grid interpolation points and the quadrature points are shown in Fig. 1.

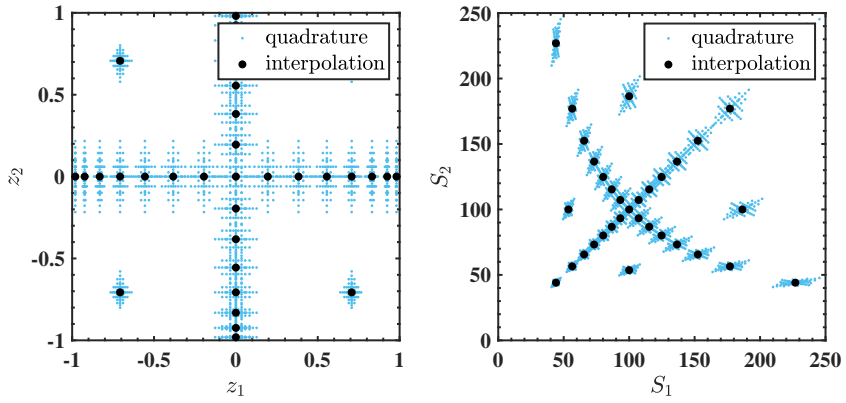

(a) (b)

Fig. 1 A schematic illustration of interpolation and quadrature points in $d = 2$; (a) in the domain of the mapped bounded variable $\mathbf{z}$; (b) in the domain of the price of underlying assets $\mathbf{S}$.

Now we can describe the procedure of iteratively interpolating the function $\overline{u}_k$ in Algorithm 1.

Followed by the Remark 1, the next result gives a sufficient condition on the well-definedness of the algorithm.

Proposition 1 *Let ε be the machine epsilon. Assume that each coordinate y_j^m of the sampling or quadrature points $\{\mathbf{y}^m\}_{m=1}^M$ of the random variable $\mathbf{Y} \sim \mathcal{N}(Q^\top(r - \boldsymbol{\delta} - \frac{1}{2}\Sigma^2\mathbf{1})\Delta t, \Lambda\Delta t)$ satisfies*

$$\max_{m=1,2,\ldots,M} |y_j^m| \le C\sqrt{\lambda_j \Delta t}, \tag{21}$$

where λ_j is the j-th diagonal element of Λ, and C is a constant. If $\beta = 1$ and L_I, L and Δt are chosen such that

$$\frac{4^{L_I+d}}{\pi^{2d}} \exp\left(2CL\sqrt{\Delta t}\sum_{j=1}^{d}\sqrt{\lambda_j}\right) \le \frac{1}{\varepsilon},$$

Algorithm 1 Pricing American option with d assets

Input: Market parameters: $\mathbf{S}_0, r, \delta_i, \sigma_i, P$
Option parameters: κ, T, option type
Transform and discretization parameters: L, K, L_I

Output: Option price V_0

Generate CGL sparse grids in $\overline{\Omega}$
Find grids in Ω, which are denoted by $\{\mathbf{z}^n\}_{n=1}^N$
Generate quadrature points $\{\mathbf{y}^m\}_{m=1}^M$ and weights $\{w_m\}_{m=1}^M$ with Gaussian density $\mathcal{N}(Q^\top(r-\boldsymbol{\delta}-\frac{1}{2}\Sigma^2\mathbf{1})\Delta t, \Lambda\Delta t)$
Dynamic programming:
Compute the payoff $H_{n,m} = H(\psi(\psi^{-1}(\mathbf{z}^n)+\mathbf{y}^m))$
Set the terminal value as $V_{n,m} = H_{n,m}$
for $k = K-1:-1:0$ **do**
  $u(\mathbf{z}^n) = \alpha\sum_{m=1}^M w_m V_{n,m} b(\mathbf{z}^n)$ where $\alpha = e^{-r\Delta t}$ is the discount factor
  if $k == 0$ **then**
    $u_0 = A(L_I+d,d)(u)(\mathbf{0})$, break
  end if
  $u_{n,m} = A(L_I+d,d)(u)\left(\psi(\psi^{-1}(\mathbf{z}^n)+\mathbf{y}^m)\right)$ ▷ Compute in parallel
  Update $V_{n,m} = \max\left(H_{n,m}, u_{n,m}/b(\psi(\psi^{-1}(\mathbf{z}^n)+\mathbf{y}^m))\right)$
end for
$V_0 = \max\left(H(\mathbf{0}), \frac{u_0}{b(\mathbf{0})}\right)$

then for all sampling or quadrature points $\mathbf{Z}_{k+1}^{n,m}$ *of* $\mathbf{Z}_{k+1}$, $n = 1,2,\ldots,N, m = 1,2,\ldots,M$, *we have*

$$b(\mathbf{Z}_{k+1}^{n,m}) > \varepsilon.$$

Proof Using (16), we have $\mathbf{Z}_{k+1}^{n,m} = \psi(\psi^{-1}(\mathbf{z}^n)+\mathbf{y}^m)$, where $\{\mathbf{z}^n\}_{n=1}^N$ are inner sparse grid interpolation points and $\{\mathbf{y}^m\}_{m=1}^M$ are sampling or quadrature points of $\mathbf{Y}$. Thus the j-th coordinate of $\mathbf{Z}_{k+1}^{n,m}$ is given by

$$Z_{k+1}^{n,m,j} = 1 - \frac{2}{1+\eta_j^{n,m}}, \quad \text{with } \eta_j^{n,m} := \frac{1+z_j^n}{1-z_j^n}\exp(2Ly_j^m).$$

For $\beta = 1$, to ensure $b(\mathbf{z}) = \prod_{j=1}^d (1-z_j^2) > \varepsilon$, it suffices to prove $\prod_{j=1}^d (1-|z_j|) > \varepsilon$. Without loss of generality, consider the case $Z_{k+1}^{n,m,j} \to 1$, i.e., $\eta_j^{n,m} \to +\infty$. Clearly, we have

$$\prod_{j=1}^d (1 - Z_{k+1}^{n,m,j}) = \prod_{j=1}^d \frac{2}{1+\eta_j^{n,m}} > \varepsilon \quad \Leftrightarrow \quad \prod_{j=1}^d \left(1+\eta_j^{n,m}\right) < \frac{2^d}{\varepsilon}.$$

Noting that $\eta_j^{n,m} \to +\infty$, the binomial expansion implies that it suffices to have $\prod_{j=1}^d \eta_j^{n,m} < \varepsilon^{-1}$. Using the relationship

$$\frac{1+\cos x}{1-\cos x} = \frac{1}{\tan^2\frac{x}{2}} \le \frac{4}{x^2} \quad \text{as } x \to 0^+,$$

d	$\tilde{N}_{full}$	$\tilde{N}_{CGL}$	N
2	961	145	81
3	29791	441	151
4	923521	1105	241
5	2.8629e+7	2433	351
6	8.8750e+8	4865	481
7	2.7513e+10	9017	631
8	8.5289e+11	15713	801
9	2.6440e+13	26017	991
10	8.1963e+14	41265	1201

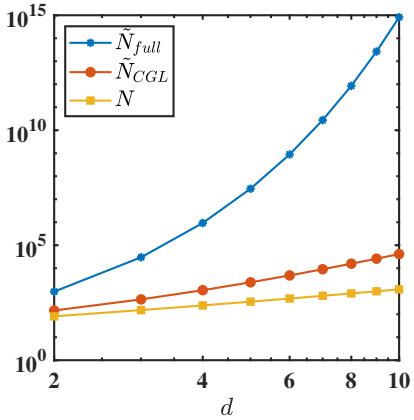

Fig. 2 The number of tensor-product full grids $\tilde{N}_{full}$, the number of Chebyshev-Gauss-Lobatto sparse grids $\tilde{N}_{CGL}$, and the number of inner sparse grids N in the d-dimensional hypercube with level $L_I = 5$.

the inequality (15), and the assumption (21), we obtain

$$\prod_{j=1}^{d}\left(\frac{1+z_j^n}{1-z_j^n}\exp(2Ly_j^m)\right) \le \prod_{j=1}^{d}\frac{1+\cos\left(\frac{\pi}{2^{\ell_j-1}}\right)}{1-\cos\left(\frac{\pi}{2^{\ell_j-1}}\right)}\exp(2CL\sqrt{\lambda_j\Delta t})$$
$$\le \left(\frac{4}{\pi^2}\right)^d 4^{\sum_{j=1}^d \ell_j - d}\exp\left(2CL\sqrt{\Delta t}\sum_{j=1}^{d}\sqrt{\lambda_j}\right).$$

Since $\sum_{j=1}^{d}\ell_i \le L_I + d$, this proves the desired assertion. □

Last, we discuss the computational complexity of Algorithm 1. By introducing the bubble function, the interpolation functions $\overline{u}_k$ vanish over the boundary. Thus, at each time step, we require N evaluations of u_k only on the inner sparse grids, where each evaluation is approximated by (18), (19) or (20) with M sampling or quadrature points. The numbers of inner sparse grids N of level $L_I = 5$ in dimension d are listed in Table 2. In comparison, the numbers for tensor-product full grids $\tilde{N}_{full}$ and CGL sparse grids with boundary points $\tilde{N}_{CGL}$ are also provided. Unlike full grids, the number of sparse grids does not increase exponentially as the dimension increases. Remarkably, the inner sparse grids account for below 3% of the CGL sparse grids in $d = 10$. This represents a dramatic reduction of the evaluation points.

4 Smoothness analysis

In this section, we analyze the smoothness of the function u_k, in order to justify the use of SGPI, thereby providing solid theoretical underpinnings of its excellent performance.

First we list several useful notations. Let $\boldsymbol{\alpha} = (\alpha_1, \ldots, \alpha_d) \in \mathbb{N}_0^d$ be the standard multi-index with $|\boldsymbol{\alpha}| = \alpha_1 + \cdots + \alpha_d$. Then $\boldsymbol{\alpha} + \boldsymbol{\gamma} := (\alpha_1 + \gamma_1, \ldots, \alpha_d + \gamma_d)$, $\boldsymbol{\alpha}! := \prod_{j=1}^{d}\alpha_j!$, and $\boldsymbol{\gamma} \preceq \boldsymbol{\alpha}$ denotes that each component of the multi-index $\boldsymbol{\gamma} = (\gamma_1, \ldots, \gamma_d)$

satisfies $\gamma_j \leq \alpha_j$. We define the differential operator $D^{\boldsymbol{\alpha}}$ by $D^{\boldsymbol{\alpha}} f := \frac{\partial^{|\boldsymbol{\alpha}|} f}{\prod_{j=1}^d \partial x_j^{\alpha_j}}$. For an open set $D \subset \mathbb{R}^d$ and $r \in \mathbb{N}$, the space $\mathcal{C}^r(\overline{D})$ denotes the space of functions with their derivatives of orders up to r being continuous on the closure $\overline{D}$ of D, i.e.,

$$\mathcal{C}^r(\overline{D}) = \{f : \overline{D} \to \mathbb{R} \mid D^{\boldsymbol{\alpha}} f \text{ continuous if } |\boldsymbol{\alpha}| \leq r\}.$$

Specially, $\mathcal{C}^r(\overline{\mathbb{R}^d})$ consists of functions $f \in \mathcal{C}^r(\mathbb{R}^d)$ such that $D^{\boldsymbol{\alpha}} f$ is bounded and uniformly continuous on $\mathbb{R}^d$ for all $|\boldsymbol{\alpha}| \leq r$ [40]. We also define $\mathcal{C}^\infty(\overline{\mathbb{R}^d})$ as the intersection of all $\mathcal{C}^r(\overline{\mathbb{R}^d})$ for $r \in \mathbb{N}$, i.e., $\mathcal{C}^\infty(\overline{\mathbb{R}^d}) := \bigcap_{r=1}^\infty \mathcal{C}^r(\overline{\mathbb{R}^d})$.

The analysis of SGPI employs the space of functions on $\overline{\Omega} := [-1, 1]^d$ with bounded mixed derivatives [28]. Let $F_d^r(\overline{\Omega})$ be the set of all functions $f : \overline{\Omega} \to \mathbb{R}$ such that $D^{\boldsymbol{\alpha}} f$ is continuous for all $\boldsymbol{\alpha} \in \mathbb{N}_0^d$ with $\alpha_i \leq r$ for all i, i.e.,

$$F_d^r(\overline{\Omega}) := \{f : \overline{\Omega} \to \mathbb{R} \mid D^{\boldsymbol{\alpha}} f \text{ continuous if } \alpha_i \leq r \text{ for all } i\}. \tag{22}$$

We equip the space $F_d^r(\overline{\Omega})$ with the norm $\|f\|_{F_d^r(\overline{\Omega})} := \max\{\|D^{\boldsymbol{\alpha}} f\|_{L^\infty(\overline{\Omega})} \mid \boldsymbol{\alpha} \in \mathbb{N}_0^d, \alpha_i \leq r\}$.

For the sake of completeness, we present in Proposition 2 the interpolation error using SGPI described in Section 3.2.

Proposition 2 ([33, Theorem 8, Remark 9]) *For $f \in F_d^r(\overline{\Omega})$, there exists a constant $c_{d,r}$ depending only on d and r such that*

$$\|A(q, d)(f) - f\|_{L^\infty(\overline{\Omega})} \leq c_{d,r} \cdot \tilde{N}^{-r} \cdot (\log \tilde{N})^{(r+1)(d-1)} \|f\|_{F_d^r(\overline{\Omega})},$$

where $\tilde{N} = \tilde{N}_{CGL}(q, d)$ is the number of CGL sparse grids.

To provide theoretical guarantees of applying SGPI, we next prove $\overline{u}_k \in F_d^r(\overline{\Omega})$ in Theorem 1. This result follows by Lemma 1 [1] and Lemma 2.

Lemma 1 ($f_{K-1} \in \mathcal{C}^\infty(\overline{\mathbb{R}^d})$) *Let g be the payoff of a put option. Then the continuation value function f_{K-1} defined in (7) is infinitely differentiable, bounded and uniformly continuous with all its derivatives up to order r for any $r \in \mathbb{N}$, i.e., $f_{K-1} \in \mathcal{C}^\infty(\overline{\mathbb{R}^d})$.*

Proof Consider the conditional expectation without the discount factor $e^{-r\Delta t}$,

$$f(\mathbf{x}) = \mathbb{E}[G(\tilde{X}_K) | \tilde{X}_{K-1} = \mathbf{x}] = \int_{\mathbb{R}^d} G(\mathbf{y}) p(\mathbf{x}, \mathbf{y}) \, \mathrm{d}\mathbf{y}, \tag{23}$$

[1] Intuitively, $\mathcal{C}^\infty(\mathbb{R}^d)$ smoothness of f_{K-1} follows directly by the fact that convolution smooths out the payoff function due to (23). However, the payoff function G of the rotated log-price is not in $L^1(\mathbb{R}^d)$, neither is the density function compactly supported. Therefore, we supplement its proof in Lemma 1 mainly by means of the dominated convergence theorem.

where $G(\cdot) = g(\phi(\cdot))$ is the payoff with respect to the rotated log-price, and $p(\mathbf{x}, \mathbf{y})$ is the density of the Gaussian distribution $\mathcal{N}(\mathbf{x} + Q^\top(r - \boldsymbol{\delta} - \frac{1}{2}\Sigma^2\mathbf{1})\Delta t, \Lambda\Delta t)$, that is,

$$p(\mathbf{x}, \mathbf{y}) = \frac{1}{(2\pi)^{d/2}\sqrt{\det(\Lambda)\Delta t}} \exp\left(-\frac{1}{2\Delta t}(\mathbf{y} - \mathbf{x} - \boldsymbol{\mu})^\top \Lambda^{-1}(\mathbf{y} - \mathbf{x} - \boldsymbol{\mu})\right) \tag{24}$$

with $\boldsymbol{\mu} = Q^\top(r - \boldsymbol{\delta} - \frac{1}{2}\Sigma^2\mathbf{1})\Delta t$. Since g is the payoff of a put option, G is bounded in $\mathbb{R}^d$. Let

$$P(\mathbf{x}) := \frac{1}{(2\pi)^{d/2}\sqrt{\det(\Lambda)\Delta t}} \exp\left(-\frac{1}{2\Delta t}(\mathbf{x} + \boldsymbol{\mu})^\top \Lambda^{-1}(\mathbf{x} + \boldsymbol{\mu})\right).$$

Then $P \in L^1(\mathbb{R}^d)$ with $\|P\|_1 = \int_{\mathbb{R}^d} P(\mathbf{x})\,\mathrm{d}\mathbf{x} = 1$. The representation (23) is equivalent to

$$f(\mathbf{x}) = G * P(\mathbf{x}),$$

where $*$ denotes the convolution operator. Then an application of [41, Proposition 8.8] implies that f is bounded and uniformly continuous in $\mathbb{R}^d$, and

$$\|f\|_{L^\infty(\mathbb{R}^d)} \le \|G\|_{L^\infty(\mathbb{R}^d)}\|P\|_{L^1(\mathbb{R}^d)} = \|G\|_{L^\infty(\mathbb{R}^d)}. \tag{25}$$

Next, we show that f has bounded first order partial derivatives for all $i \in \{1, 2, \ldots, d\}$, and

$$\frac{\partial f}{\partial x_i}(\mathbf{x}) = G * \frac{\partial P}{\partial x_i}(\mathbf{x}). \tag{26}$$

For any fixed $\mathbf{x}_0 \in \mathbb{R}^d$, $i \in \{1, 2, \ldots, d\}$,

$$\frac{\partial p}{\partial x_i}(\mathbf{x}_0, \mathbf{y}) = \lim_{\mathbf{x}_n \to \mathbf{x}_0} q_{i,n}(\mathbf{y}), \quad \text{with } q_{i,n}(\mathbf{y}) = \frac{p(\mathbf{x}_n, \mathbf{y}) - p(\mathbf{x}_0, \mathbf{y})}{x_{i,n} - x_{i,0}}.$$

Note that the Gaussian density $p(\mathbf{x}, \mathbf{y})$ has bounded partial derivatives $\frac{\partial p}{\partial x_i}(\mathbf{x}, \mathbf{y})$ for all $\mathbf{x}, \mathbf{y}$ and $i \in \{1, 2, \ldots, d\}$, we derive

$$\begin{aligned}
\frac{\partial f}{\partial x_i}(\mathbf{x}_0) &= \lim_{\mathbf{x}_n \to \mathbf{x}_0} \frac{f(\mathbf{x}_n) - f(\mathbf{x}_0)}{x_{i,n} - x_{i,0}} \\
&= \lim_{\mathbf{x}_n \to \mathbf{x}_0} \int_{\mathbb{R}^d} G(\mathbf{y}) \frac{p(\mathbf{x}_n, \mathbf{y}) - p(\mathbf{x}_0, \mathbf{y})}{x_{i,n} - x_{i,0}}\,\mathrm{d}\mathbf{y} \\
&= \lim_{\mathbf{x}_n \to \mathbf{x}_0} \int_{\mathbb{R}^d} G(\mathbf{y}) q_{i,n}(\mathbf{y})\,\mathrm{d}\mathbf{y}.
\end{aligned} \tag{27}$$

Since G is bounded and $p(\mathbf{x}, \mathbf{y})$ decays as $\mathcal{O}(e^{-\|\mathbf{y}\|_2^2})$ at infinity for fixed $\mathbf{x}$, this indicates that the integrand $G(\mathbf{y})q_{i,n}(\mathbf{y})$ is bounded by some Lebesgue integrable function for all n. Consequently, the dominated convergence theorem implies that one can interchange the limit and integral in the last equality of (27), which leads to

$$\frac{\partial f}{\partial x_i}(\mathbf{x}_0) = \int_{\mathbb{R}^d} G(\mathbf{y}) \frac{\partial p}{\partial x_i}(\mathbf{x}_0, \mathbf{y})\,\mathrm{d}\mathbf{y} = G * \frac{\partial P}{\partial x_i}(\mathbf{x}_0).$$

Then [41, Proposition 8.8] implies that $\frac{\partial f}{\partial x_i}$ is bounded and uniformly continuous in $\mathbb{R}^d$, and moreover, there holds

$$\left\|\frac{\partial f}{\partial x_i}\right\|_{L^\infty(\mathbb{R}^d)} \le \|G\|_{L^\infty(\mathbb{R}^d)} \left\|\frac{\partial P}{\partial x_i}\right\|_{L^1(\mathbb{R}^d)}.$$

This, together with the dominated convergence theorem, leads to the formula for the second order partial derivatives,

$$\frac{\partial^2 f}{\partial x_j \partial x_i}(\mathbf{x}) = G * \frac{\partial^2 P}{\partial x_j \partial x_i}(\mathbf{x}).$$

Note that for fixed $\mathbf{x}$, the function

$$\frac{\partial p}{\partial x_i}(\mathbf{x},\mathbf{y}) = -\frac{(x_i - y_i + \mu_i)}{\lambda_i \Delta t} p(\mathbf{x},\mathbf{y})$$

decays as $\mathcal{O}(\mathbf{y} e^{-\|\mathbf{y}\|_2^2})$ at infinity. Combining with [41, Proposition 8.8], we obtain $\frac{\partial^2 f}{\partial x_j \partial x_i}$ is bounded and uniformly continuous on $\mathbb{R}^d$, and

$$\left\| \frac{\partial^2 f}{\partial x_j \partial x_i} \right\|_{L^\infty(\mathbb{R}^d)} \leq \|G\|_{L^\infty(\mathbb{R}^d)} \left\| \frac{\partial^2 P}{\partial x_j \partial x_i} \right\|_{L^1(\mathbb{R}^d)}.$$

Repeating the argument yields the boundedness and uniform continuity of the partial derivatives of f up to the order r for any $r \in \mathbb{N}$. Therefore, $f_{K-1} \in \mathcal{C}^\infty(\overline{\mathbb{R}^d})$. □

Lemma 2 ($f_k \in \mathcal{C}^\infty(\overline{\mathbb{R}^d})$ for $k = 0, 1, \ldots, K-1$) *Let g be the payoff of a put option. Then the continuation value functions $\{f_k\}_{k=0}^{K-1}$ defined in (7) are infinitely differentiable, bounded and uniformly continuous with all its derivatives up to the order r for any $r \in \mathbb{N}$, i.e., $f_k \in \mathcal{C}^\infty(\overline{\mathbb{R}^d})$ for $k = 0, 1, \ldots, K-1$.*

Proof Let the value at t_{k+1} be

$$V_{k+1}(\mathbf{y}) = \max\left(G(\mathbf{y}), f_{k+1}(\mathbf{y})\right), \quad \text{for } k = 0, 1, \ldots, K-2,$$

where $G(\cdot) = g(\phi(\cdot))$ is bounded for a put option. By (25), f_{K-1} is bounded. Hence, V_{K-1} is bounded in $\mathbb{R}^d$. Using the argument of Lemma 1, we obtain

$$f_{K-2}(\mathbf{x}) = e^{-r\Delta t}\mathbb{E}[V_{K-1}(\tilde{\mathbf{X}}_{K-1})|\tilde{\mathbf{X}}_{K-2} = \mathbf{x}] = e^{-r\Delta t} V_{K-1} * P(\mathbf{x})$$

is infinitely differentiable, bounded and uniformly continuous with all its derivatives up to the order r for any $r \in \mathbb{N}$. Since $\|f_{K-2}\|_{L^\infty(\mathbb{R}^d)} \leq e^{-r\Delta t}\|V_{K-1}\|_{L^\infty(\mathbb{R}^d)}\|P\|_{L^1(\mathbb{R}^d)}$, the value V_{K-2} is bounded in $\mathbb{R}^d$. Similarly, we can obtain $f_k \in \mathcal{C}^\infty(\overline{\mathbb{R}^d})$ for all $k = 0, 1, \ldots, K-1$. □

Using the smoothness of the continuation value functions in $\mathbb{R}^d$, now we can establish the smoothness of the extended interpolation function $\overline{u}_k$ in the bounded domain $\overline{\Omega} = [-1, 1]^d$.

Theorem 1 ($\overline{u}_k \in F_d^r(\overline{\Omega})$ for $k = 0, 1, \ldots, K-1$) *Let g be the payoff of a put option. Let $u_k : \Omega \to \mathbb{R}$ be the function defined in (12) with $u_k(\mathbf{z}) = f_k(\psi^{-1}(\mathbf{z}))b(\mathbf{z})$. Let $b(\cdot)$ be the bubble function of the form (11) and ψ^{-1} be the mapping between unbounded and bounded domains defined in (8). If $\beta \geq r$ with $r \in \mathbb{N}$, then u_k can be extended to $\overline{u}_k : \overline{\Omega} \to \mathbb{R}$ such that $\overline{u}_k$ has bounded mixed derivatives up to order r, i.e.,*

$$\overline{u}_k \in F_d^r(\overline{\Omega}), \quad \text{for } k = 0, 1, \ldots, K-1.$$

Furthermore, for $\boldsymbol{\alpha} \in \mathbb{N}_0^d$ with $\alpha_j \leq r$, there holds

$$\begin{aligned} D^{\boldsymbol{\alpha}}\overline{u}_k(\mathbf{z}) = \sum_{\substack{\boldsymbol{\gamma}+\boldsymbol{\zeta}=\boldsymbol{\alpha} \\ \boldsymbol{\gamma}\preceq\boldsymbol{\alpha}, \boldsymbol{\zeta}\preceq\boldsymbol{\alpha}}} \frac{\boldsymbol{\alpha}!}{\boldsymbol{\gamma}!\boldsymbol{\zeta}!} D^{\boldsymbol{\gamma}} f_k \prod_{j=1:d,\gamma_j=0} \left((1-z_j^2)^{\beta-\zeta_j} Q_{\zeta_j}(z_j)\right) \\ \times \prod_{j=1:d,\gamma_j\geq 1} \left(\frac{1}{L}(1-z_j^2)^{\beta-\zeta_j-\gamma_j} Q_{\zeta_j}(z_j) P_{\gamma_j}(z_j)\right), \end{aligned} \tag{28}$$

where Q_{ζ_j} and P_{γ_j} are univariate polynomials of degrees ζ_j and $\gamma_j - 1$ defined on $[-1, 1]$.

Proof First, for the multi-index $\boldsymbol{\alpha}$ with $|\boldsymbol{\alpha}| = 0$,

$$D^{\boldsymbol{\alpha}} u_k(\mathbf{z}) = u_k(\mathbf{z}) = F_k(\mathbf{z}) b(\mathbf{z}) = f_k(\psi^{-1}(\mathbf{z})) b(\mathbf{z})$$

is continuous and bounded in Ω due to the continuity and boundedness of f_k in Lemma 2. Since u_k approaches zero as $\mathbf{z} \to \partial\Omega$, we can define $\overline{u}_k|_{\partial\Omega} = 0$, and $\overline{u}_k|_{\Omega} = u_k$ for each $k = 0, 1, \ldots, K-1$. Then $\overline{u}_k$ is continuous in the closure $\overline{\Omega}$. The following argument holds for all $k = 0, 1, \ldots, K-1$. Thus, we drop the subscript k and denote $u := u_k$, $F := F_k$ and $f := f_k$. For any multi-index $\boldsymbol{\alpha} \in \mathbb{N}_0^d$, Leibniz's rule implies

$$D^{\boldsymbol{\alpha}} u = \sum_{\substack{\boldsymbol{\gamma}+\boldsymbol{\zeta}=\boldsymbol{\alpha} \\ \boldsymbol{\gamma} \preceq \boldsymbol{\alpha}, \boldsymbol{\zeta} \preceq \boldsymbol{\alpha}}} \frac{\boldsymbol{\alpha}!}{\boldsymbol{\gamma}!\boldsymbol{\zeta}!} D^{\boldsymbol{\gamma}} F \cdot D^{\boldsymbol{\zeta}} b. \tag{29}$$

For any fixed $r \in \mathbb{N}$, pick $\beta \geq r$. Consider a multi-index $\boldsymbol{\alpha}$ with $\alpha_i \leq r$, $i = 1, \ldots, d$. Let $b(\mathbf{z}) = \prod_{j=1}^d b_j(z_j)$ with $b_j(z_j) = (1 - z_j^2)^{\beta}$. Then direct computation yields

$$D^{\boldsymbol{\zeta}} b = \prod_{j=1}^d \frac{\mathrm{d}^{\zeta_j} b_j}{\mathrm{d} z_j^{\zeta_j}} \quad \text{with} \quad \frac{\mathrm{d}^i b_j}{\mathrm{d} z_j^i} := (1 - z_j^2)^{\beta - i} Q_i(z_j), \tag{30}$$

where $Q_i(z_j)$ is a univariate polynomial of degree i for all $i = 0, 1, \ldots, r$. Note that $F(\mathbf{z}) = f(\psi^{-1}(\mathbf{z}))$ depends only on z_j through x_j with $\mathbf{x} = \psi^{-1}(\mathbf{z})$. Then we have

$$\begin{aligned} D^{\boldsymbol{\gamma}} F = D^{\boldsymbol{\gamma}} \left(f(\psi^{-1}(\mathbf{z})) \right) = \frac{\partial^{|\boldsymbol{\gamma}|} f}{\prod_{j=1}^d \partial x_j^{\gamma_j}} \prod_{j=1: d, \gamma_j \geq 1} \frac{\mathrm{d}^{\gamma_j} x_j}{\mathrm{d} z_j^{\gamma_j}} \quad \text{with} \\ \frac{\mathrm{d}^{\ell} x_j}{\mathrm{d} z_j^{\ell}} := \frac{1}{L} (1 - z_j^2)^{-\ell} P_{\ell}(z_j), \end{aligned} \tag{31}$$

where $P_\ell(z_j)$ is a univariate polynomial of degree $\ell - 1$ for all $\ell = 1, 2, \ldots, r$. Combining the last three identities yields the assertion (28). Since $\beta - \zeta_j - \gamma_j = \beta - \alpha_j \geq 0$, by Lemma 2, we deduce that $D^{\boldsymbol{\alpha}} u_k$ is bounded. By defining the continuous extension of $D^{\boldsymbol{\alpha}} u_k$ using (28), we obtain that $\overline{u}_k \in F_d^r(\overline{\Omega})$ for $k = 0, 1, \ldots, K-1$. □

To bound $\overline{u}_k$ in the $F_d^r(\overline{\Omega})$ norm, we need suitable estimates of polynomials Q_i and P_ℓ in (28).

Lemma 3 *For fixed $\beta \geq r$ with $r \in \mathbb{N}$, $i = 1, 2, \ldots, r$ and $\ell = 1, 2, \ldots, r$, the polynomials Q_i defined in (30) and P_ℓ defined in (31) satisfy the following estimates*

$$\|Q_i\|_{L^\infty([-1,1])} \leq \prod_{n=0}^{i-1} \left(n^2 + 2(\beta - n) \right) \quad \text{and} \quad \|P_\ell\|_{L^\infty([-1,1])} \leq \prod_{n=0}^{\ell-1} (n^2 + 1). \tag{32}$$

Proof By (30), $\|Q_0\|_{L^\infty([-1,1])} = 1$. Using the identity $\frac{\mathrm{d}}{\mathrm{d} z_j} \left(\frac{\mathrm{d}^{i-1} b_j}{\mathrm{d} z_j^{i-1}} \right) = \frac{\mathrm{d}^i b_j}{\mathrm{d} z_j^i}$, for $i > 1$, and the defining identity in (30), we obtain

$$\frac{\mathrm{d}}{\mathrm{d} z_j} \left((1 - z_j^2)^{\beta - i + 1} Q_{i-1}(z_j) \right) = (1 - z_j^2)^{\beta - i} Q_i(z_j).$$

Dividing both sides by $(1 - z_j^2)^{\beta - i}$ after taking derivative over the left hand side, we obtain

$$(\beta - i + 1)(-2 z_j) Q_{i-1}(z_j) + (1 - z_j^2) Q_{i-1}'(z_j) = Q_i(z_j).$$

By the triangular inequality, we derive

$$\|Q_i\|_{L^\infty([-1,1])} \leq 2(\beta - i + 1)\|Q_{i-1}\|_{L^\infty([-1,1])} + \|Q'_{i-1}\|_{L^\infty([-1,1])}. \tag{33}$$

Since Q_{i-1} is a polynomial of degree $i-1$ defined on $[-1,1]$, a direct application of the Markov brothers' inequality [42, p. 300] yields

$$\|Q'_{i-1}\|_{L^\infty([-1,1])} \leq (i-1)^2\|Q_{i-1}\|_{L^\infty([-1,1])}.$$

Plugging this estimate into (33) leads to the recurrence relation

$$\|Q_i\|_{L^\infty([-1,1])} \leq \Big((i-1)^2 + 2(\beta - (i-1))\Big)\|Q_{i-1}\|_{L^\infty([-1,1])}. \tag{34}$$

Upon noting $\|Q_0\|_{L^\infty([-1,1])} = 1$, we derive the desired estimate on Q_i. The estimate on P_i follows similarly. For $\ell = 1$, $\|P_1\|_{L^\infty([-1,1])} = 1$. For $\ell > 1$, using (31), we obtain

$$\frac{\mathrm{d}}{\mathrm{d}z_j}\left(\frac{\mathrm{d}^{\ell-1}x_j}{\mathrm{d}z_j^{\ell-1}}\right) = \frac{\mathrm{d}}{\mathrm{d}z_j}\left(\frac{1}{L}(1-z_j^2)^{-\ell+1}P_{\ell-1}(z_j)\right) = \frac{1}{L}(1-z_j^2)^{-\ell}P_\ell(z_j) = \frac{\mathrm{d}^\ell x_j}{\mathrm{d}z_j^\ell}.$$

This implies

$$2(\ell-1)z_jP_{\ell-1}(z_j) + (1-z_j^2)P'_{\ell-1}(z_j) = P_\ell(z_j).$$

Since $P_{\ell-1}$ is a polynomial of degree $\ell-2$, by the triangular inequality and the Markov brothers' inequality, we obtain the recurrence relation

$$\|P_\ell\|_{L^\infty([-1,1])} \leq \Big((\ell-1)^2 + 1\Big)\|P_{\ell-1}\|_{L^\infty([-1,1])}. \tag{35}$$

Together with the identity $\|P_1\|_{L^\infty([-1,1])} = 1$, we prove the desired assertion on P_ℓ. □

We now estimate the norms $\|D^{\boldsymbol{\alpha}}u_k\|_{L^\infty(\overline{\Omega})}$ in terms of suitable mixed norms of f. Here,

$$\|f\|_{mix,r} := \max\left\{\left\|\frac{\partial^{|\boldsymbol{\alpha}|}f}{\prod_{j=1}^d \partial x_j^{\alpha_j}}\right\|_{L^\infty(\mathbb{R}^d)} : \mathbf{x}\in\mathbb{R}^d, \boldsymbol{\alpha}\in\mathbb{N}_0^d \text{ with } \alpha_j \leq r\right\}.$$

Theorem 2 (Upper bounds on $\|\overline{u}_k\|_{F_d^1(\overline{\Omega})}$ and $\|\overline{u}_k\|_{F_d^2(\overline{\Omega})}$ for $k = 0, 1, \ldots, K-1$) *Let g be the payoff of a put option, and $u_k : \Omega \to \mathbb{R}$ the function defined in (12) with $u_k(\mathbf{z}) = f_k(\psi^{-1}(\mathbf{z}))b(\mathbf{z})$. Let $b(\cdot)$ be the bubble function of the form (11) and ψ^{-1} the mapping between unbounded and bounded domains defined in (8). Then for $k \in \{0, 1, \ldots, K-1\}$, if $\beta = 1$ in (11), there holds*

$$\|\overline{u}_k\|_{F_d^1(\overline{\Omega})} \leq \left(2 + \frac{1}{L}\right)^d \|f_k\|_{mix,1}.$$

If $\beta = 2$ in (11), then

$$\|\overline{u}_k\|_{F_d^2(\overline{\Omega})} \leq \left(24 + \frac{12}{L}\right)^d \|f_k\|_{mix,2}.$$

Proof Combining (28) with (32) leads to

$$\|D^{\boldsymbol{\alpha}}\overline{u}_k\|_{L^\infty(\overline{\Omega})} \leq \sum_{\substack{\boldsymbol{\gamma}+\boldsymbol{\zeta}=\boldsymbol{\alpha}\\ \boldsymbol{\gamma}\preceq\boldsymbol{\alpha},\boldsymbol{\zeta}\preceq\boldsymbol{\alpha}}} \frac{\boldsymbol{\alpha}!}{\boldsymbol{\gamma}!\boldsymbol{\zeta}!}\|D^{\boldsymbol{\gamma}}f_k\|_{L^\infty(\mathbb{R}^d)} \prod_{j=1:d,\gamma_j=0} \|Q_{\zeta_j}\|_{L^\infty([-1,1])} \tag{36}$$

$$\times \prod_{j=1:d,\gamma_j\geq 1}\left(\frac{1}{L}\|Q_{\zeta_j}\|_{L^\infty([-1,1])}\|P_{\gamma_j}\|_{L^\infty([-1,1])}\right).$$

It follows from Lemma 3 that

$$\|Q_0\|_{L^\infty([-1,1])}=1,\quad \|Q_1\|_{L^\infty([-1,1])}\leq 2\beta,\quad \|Q_2\|_{L^\infty([-1,1])}\leq (2\beta-1)2\beta,$$
$$\|P_1\|_{L^\infty([-1,1])}=1,\quad \|P_2\|_{L^\infty([-1,1])}\leq 2.$$

Next, we deduce the following estimates from (36). If $\beta=1$, consider the multi-index $\boldsymbol{\alpha}$ with $\alpha_j\in\{0,1\}$ for $j=1,2,\ldots,d$, then

$$\begin{aligned}\|D^{\boldsymbol{\alpha}}\overline{u}_k\|_{L^\infty(\overline{\Omega})} &\leq \sum_{\substack{\boldsymbol{\gamma}+\boldsymbol{\zeta}=\boldsymbol{\alpha}\\ \boldsymbol{\gamma}\preceq\boldsymbol{\alpha},\boldsymbol{\zeta}\preceq\boldsymbol{\alpha}}}\frac{\boldsymbol{\alpha}!}{\boldsymbol{\gamma}!\boldsymbol{\zeta}!}\|f_k\|_{mix,1}\prod_{j=1:d,\gamma_j=0}2\beta\prod_{j=1:d,\gamma_j\geq 1}\frac{1}{L}\\ &= \sum_{\substack{\boldsymbol{\gamma}+\boldsymbol{\zeta}=\boldsymbol{\alpha}\\ \boldsymbol{\gamma}\preceq\boldsymbol{\alpha},\boldsymbol{\zeta}\preceq\boldsymbol{\alpha}}}2^{|\boldsymbol{\zeta}|}\left(\frac{1}{L}\right)^{|\boldsymbol{\gamma}|}\|f_k\|_{mix,1}=\left(2+\frac{1}{L}\right)^{|\boldsymbol{\alpha}|}\|f_k\|_{mix,1}\\ &\leq \left(2+\frac{1}{L}\right)^d\|f_k\|_{mix,1}.\end{aligned}$$

If $\beta=2$, consider the multi-index $\boldsymbol{\alpha}$ with $\alpha_j\in\{0,1,2\}$ for $j=1,2,\ldots,d$, an application of the trinomial expansion implies

$$\begin{aligned}&\|D^{\alpha}\overline{u}_k\|_{L^\infty(\overline{\Omega})}\\ &\leq \|f_k\|_{mix,2}\sum_{\substack{\boldsymbol{\gamma}+\boldsymbol{\zeta}=\boldsymbol{\alpha}\\ \boldsymbol{\gamma}\preceq\boldsymbol{\alpha},\boldsymbol{\zeta}\preceq\boldsymbol{\alpha}}}\frac{\boldsymbol{\alpha}!}{\boldsymbol{\gamma}!\boldsymbol{\zeta}!}\prod_{j=1:d,\gamma_j=0}(2\beta-1)2\beta\prod_{j=1:d,\gamma_j=1}\frac{1}{L}(2\beta)\prod_{j=1:d,\gamma_j=2}\frac{1}{L}\cdot 2\\ &\leq 2^d\left(2\beta(2\beta-1)+\frac{2\beta}{L}+\frac{2}{L}\right)^d\|f_k\|_{mix,2}=\left(24+\frac{12}{L}\right)^d\|f_k\|_{mix,2}.\end{aligned}$$

This completes the proof of the theorem. □

In Theorem 2, we only consider the cases $\beta=1$ and $\beta=2$, and both can overcome the curse of dimensionality by means of SGPI while maintaining a relatively small upper bound of the functional norm. Clearly, higher order mixed derivatives of the interpolation function u_k have larger upper bounds.

5 Numerical experiments

In this section, we illustrate the efficiency and robustness of the proposed quadrature and sparse grid interpolation scheme, i.e., Algorithm 1, for pricing high-dimensional American options. We present pricing results up to dimension 16. The accuracy of the option price $\hat{V}$ obtained by Algorithm 1 is measured in the relative error defined by

$$e=|\hat{V}-V^\dagger|/V^\dagger,$$

where $V^\dagger$ is the reference price, either taken from literature or computed to meet a certain tolerance. The results show that the relative errors decay geometrically as the number of interpolation points increase, and the convergence rate is almost independent of the dimension d. The comparison of various quadrature methods is also

included. The implementation of sparse grids is based on the Sparse Grids MATLAB Kit, a MATLAB toolbox for high-dimensional quadrature and interpolation [39]. The computations were performed by MATLAB R2022b with 32 CPU cores (with 4GB memory per core) using research computing facilities offered by Information Technology Services, The University of Hong Kong. The codes for the numerical experiments can be founded in https://github.com/jiefeiy/multi-asset-American-option/tree/main.

5.1 American basket option pricing up to dimension 16

The examples are taken from [5], where pricing American options up to 6 assets by the FEM was investigated. For each d-dimensional problem, the setting of these examples are $S_0^i = \kappa = 100$, $T = 0.25$, $r = 0.03$, $\delta_i = 0$, $\sigma_i = 0.2$, $P = (\rho_{ij})_{d\times d}$ with $\rho_{ij} = 0.5$ for $i \neq j$. The prices of arithmetic basket options with $d = 2, 3, \ldots, 12$ underlying assets are listed in Table 1, where the last column gives the reference price $V^\dagger_{\text{Amer}}$ of American options reported in [5], where the relative error is 0.758% for pricing a 6-d American geometric put option.

To further illustrate the efficiency of the algorithm in high dimensions, we consider pricing the geometric basket put options as benchmarks, which can be reduced to a one-dimensional problem. Thus, highly accurate prices are available using one-dimensional quadrature and interpolation scheme. Indeed, the price of the d-dimensional problem equals that of the one-dimensional American put option with initial price, volatility, and dividend yield given by

$$\hat{S}_0 = \Big(\prod_{i=1}^{d} S_0^i\Big)^{1/d}, \quad \hat{\sigma} = \frac{1}{d}\sqrt{\sum_{i,j}\sigma_i\sigma_j\rho_{ij}}, \quad \hat{\delta} = \frac{1}{d}\sum_{i=1}^{d}\Big(\delta_i + \frac{\sigma_i^2}{2}\Big) - \frac{\hat{\sigma}^2}{2},$$

respectively. The prices of geometric basket options with $d = 2, 3, \ldots, 16$ underlying assets are listed in Table 2, where the reference Bermudan prices $V^\dagger_{\text{Ber}}$ with 50 times steps with accuracy up to 10^{-6} are calculated using one-dimensional quadrature and interpolation scheme. The last column of Table 2 are the reference prices $V^\dagger_{\text{Amer}}$ of American options reported in [5] priced by the reduced one-dimensional problem.

5.2 Convergence of interpolation for Bermudan options

To verify the convergence rate of the SGPI, we consider 50-times exercisable Bermudan basket put option on the geometric average of d assets. To avoid the influence of quadrature errors, sparse grid quadrature with level 4 Genz-Keister knots is applied to ensure the small approximation errors. Fig. 3 shows the convergence for different dimension d. These plots show that for a fixed number of inner sparse grids N, the relative error do increase with the dimension d, but the convergence rate is nearly independent of the dimension, confirming the theoretical prediction in Section 4.

Table 1 The prices for the arithmetic basket put option on d assets with $\beta = 1$, $L = 2$, and $K = 50$, using sparse grid quadrature with level 4 Genz-Keister knots. The relative errors in the brackets are compared with the American price $V^{\dagger}_{\text{Amer}}$.

	Sparse grid interpolation level L_I					
d	3	4	5	6	7	$V^{\dagger}_{\text{Amer}}$ [1]
2	2.9193	3.1397	3.1330	3.1269	3.1388	3.13955
	(7.02e-2)	(3.52e-5)	(2.07e-3)	(4.03e-3)	(2.30e-4)	
3	2.8649	2.9533	2.9300	2.9304	2.9463	2.94454
	(2.71e-2)	(2.96e-3)	(4.95e-3)	(4.81e-3)	(5.83e-4)	
4	2.8429	2.8547	2.8232	2.8311		2.84019
	(9.42e-4)	(5.11e-3)	(5.98e-3)	(3.22e-3)		
5	2.8271	2.7906	2.7601	2.7710		2.77193
	(1.99e-2)	(6.74e-3)	(4.25e-3)	(3.26e-4)		
6	2.8129	2.7455	2.7191	2.7319		2.71838
	(3.48e-2)	(9.96e-3)	(2.60e-4)	(4.97e-3)		
7	2.7988	2.7140	2.6913	2.7052		
8	2.7841	2.6908	2.6718			
9	2.7720	2.6690	2.6553			
10	2.7599	2.6498	2.6428			
11	2.7472	2.6331	2.6334			
12	2.7345	2.6210	2.6256			

[1] Reference values are reported in [5].

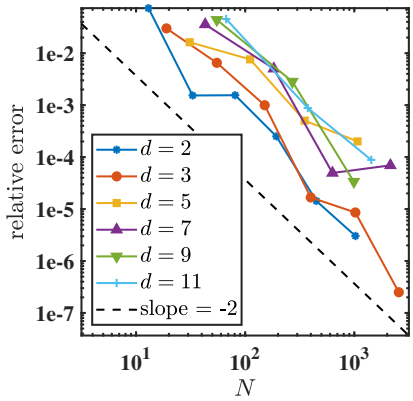

Fig. 3 The relative error w.r.t the number of inner sparse grid interpolation points N in dimension d with $\beta = 1$, $L = 2$, and $K = 50$.

5.3 Comparison of quadrature

Now we showcase the performance of Algorithm 1 with different quadrature methods, to demonstrate the flexibility of high-dimensional quadrature rules. Since the pointwise evaluations on the inner sparse grids for interpolation are obtained via quadrature methods, cf. Section 3.3, we present the error of the pricing with three kinds of sparse grid quadrature, the random quasi-Monte Carlo (RQMC) method with scramble Sobol

Table 2 The prices for the geometric basket put option on d assets with $\beta = 1$, $L = 2$, and $K = 50$, using sparse grid quadrature with level 4 Genz-Keister knots. The relative errors in the brackets are compared with 50-times exercisable Bermudan price $V^{\dagger}_{\text{Ber}}$.

	Sparse grid interpolation level L_I						
d	3	4	5	6	7	$V^{\dagger}_{\text{Ber}}$	$V^{\dagger}_{\text{Amer}}$ [1]
2	2.9489	3.1880	3.1880	3.1839	3.1831	3.18310	3.18469
	(7.36e-2)	(1.53e-3)	(1.55e-3)	(2.51e-4)	(1.43e-5)		
3	2.9130	3.0226	3.0060	3.0029	3.0030	3.00299	3.00448
	(3.00e-2)	(6.53e-3)	(9.96e-4)	(1.67e-5)	(8.59e-6)		
4	2.9028	2.9314	2.9103	2.9088		2.90836	2.90980
	(1.91e-3)	(7.94e-3)	(6.75e-4)	(1.42e-4)			
5	2.8963	2.8716	2.8514	2.8505		2.84994	2.85135
	(1.63e-2)	(7.60e-3)	(5.03e-4)	(2.00e-4)			
6	2.8889	2.8283	2.8110	2.8107		2.81026	2.81165
	(2.80e-2)	(6.40e-3)	(2.74e-4)	(1.65e-4)			
7	2.8810	2.7955	2.7817	2.7817		2.78155	
	(3.57e-2)	(5.03e-3)	(4.95e-5)	(6.93e-5)			
8	2.8725	2.7718	2.7599			2.75980	
	(4.08e-2)	(4.34e-3)	(3.47e-5)				
9	2.8631	2.7505	2.7428			2.74275	
	(4.39e-2)	(2.84e-3)	(3.37e-5)				
10	2.8525	2.7320	2.7292			2.72904	
	(4.52e-2)	(1.08e-3)	(6.66e-5)				
11	2.8412	2.7154	2.7180			2.71776	
	(4.54e-2)	(8.79e-4)	(8.83e-5)				
12	2.8294	2.7000	2.7085			2.70832	
	(4.47e-2)	(3.09e-3)	(7.74e-5)				
13	2.8175	2.6855				2.70031	
	(4.34e-2)	(5.47e-3)					
14	2.8043	2.6720				2.69342	
	(4.12e-2)	(7.95e-3)					
15	2.7910	2.6597				2.68743	
	(3.85e-2)	(1.03e-2)					
16	2.7784	2.6502				2.68218	
	(3.59e-2)	(1.19e-2)					

[1] Reference values are reported in [5].

sequence, and the state-of-art preintegration strategy for the integrand with 'kinks' (discontinuity of gradient).

Sparse grid quadrature: We first show the relative errors of pricing using (20) in Fig. 4b, for three types of sparse grids, i.e., Gauss-Hermite, Genz-Keister, and normal Leja points for integration with respect to the Gaussian density. The theoretical convergence of the sparse grid quadrature are limited to functions with bounded mixed derivatives, which is not satisfied by $v^{\mathbf{z}}_{k+1}(\cdot)$ defined in (17). Nonetheless, the success of sparse grid quadrature for computing risk-neutral expectations has been observed in the literatures [30, 31, 43]. Fig. 4a shows the $L^{\infty}(\overline{\Omega})$-error of approximating F_{K-1} by sparse grid quadrature, where the exact values correspond to the price of European options with expiration time Δt. We observe that the quadrature errors in Fig. 4a seems much larger than the relative errors shown in Fig. 4b, which seems impausible at the first glance since the latter is poluted by many errors including the former.

We find that the quadrature errors are large only near the free interface, which is a $(d-1)$-dimensional manifold in the d-dimensional problem, and hence do not result in a heavy impact on the relative errors depicted in Fig. 4b.

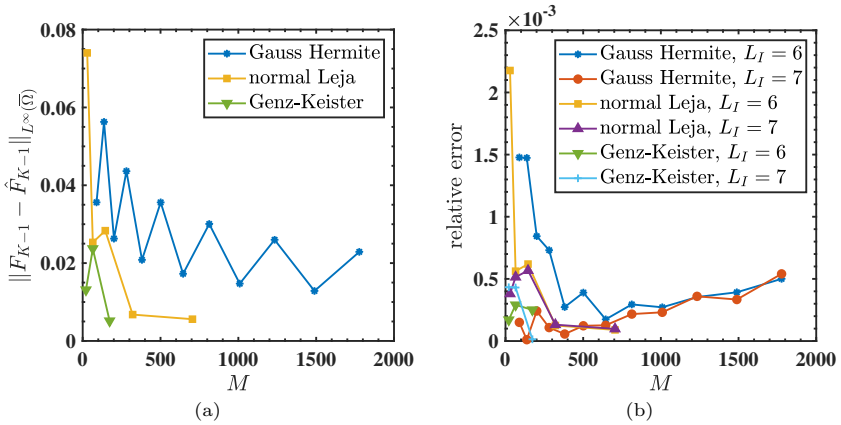

Fig. 4 (a) The $L^\infty(\overline{\Omega})$-error w.r.t. the number of quadrature points M for approximating F_{K-1} by sparse grid quadrature rules in dimension 2. (b) The relative error for pricing the Bermudan geometric basket put option in dimension 2 with $\beta = 1$, $L = 2$, and $K = 50$.

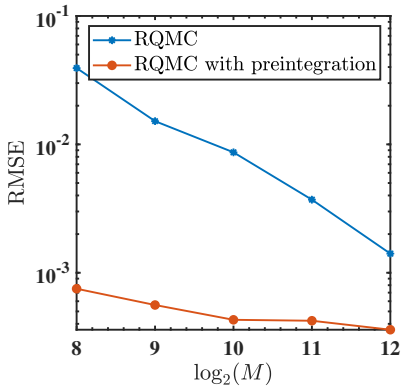

Fig. 5 The RMSE w.r.t. the number of scrambled Sobol points M for pricing the 5-d Bermudan geometric basket put option with $L_I = 6$, $\beta = 1$, $L = 2$, and $K = 50$.

RQMC and RQMC with preintegration: To show the convergence with respect to the number of quadrature points M, we use randomized quasi-Monte Carlo (RQMC) with the scramble Sobol sequence for quadrature. QMC and RQMC have been widely applied to option pricing problems for computing high-dimensional integrals [44–46]. The max function in (17) introduces a 'kink', which decreases the

efficiency of sparse grid quadrature or QMC. For functions with 'kinks', the preintegration strategy or conditional sampling are developed [47, 48]. Fig. 5 shows the root mean square error (RMSE) of Bermudan option pricing with respect to the number of quadrature points M in a 5-d problem, where we use 20 independent replicates to estimate RMSE by RMSE $= \sqrt{\frac{1}{20}\sum_{i=1}^{20}(\hat{V}^{(i)} - V^{\dagger})^2}$.

5.4 Robustness

To test the robustness of Algorithm 1, we repeat the experiments for various values of the parameter β occurred in the definition of the bubble function (11), the scale parameter L introduced in the scaled tanh map (8), and the number of time steps K. The corresponding results are shown in Fig. 6a, Fig. 6b, and Fig. 6c. We test with the example of pricing Bermudan or American geometric basket put options, where the prices are listed in Table 2.

Fig. 6a shows the convergence of relative errors for $\beta = 1, 2, 3, 4, 5$. Theoretically we have only provided the upper bounds of $\|\overline{u}_k\|_{F_d^1(\overline{\Omega})}$ and $\|\overline{u}_k\|_{F_d^2(\overline{\Omega})}$ in Theorem 2. The relative errors with respect to the chosen scale parameter L are displayed in Fig. 6b. The smallest relative error is observed for $L = 3.5$. In practice, as mentioned in Section 3.1, the parameter $L > 0$ is determined such that the transformed interpolation points are distributed alike to the asset prices. Theorem 2 implies that the scale parameter L should not be too small, and Proposition 1 implies that L should not be too large. The time discretization always arises when using the price of K-times

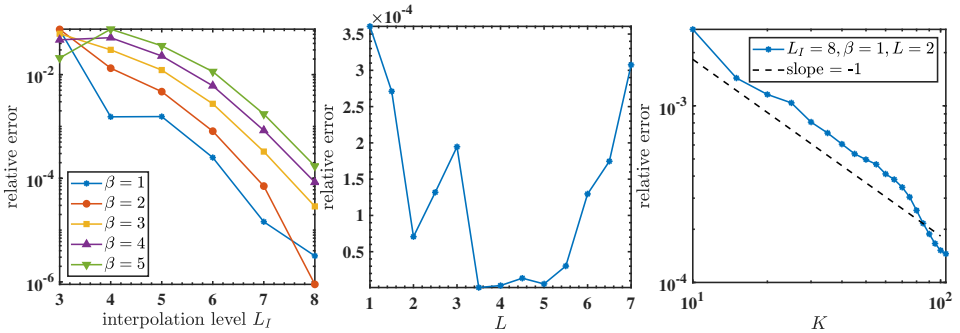

Fig. 6 (a) The relative errors decay for various β for pricing the Bermudan geometric basket put option in dimension 2 with $L = 2$ and $K = 50$. (b) The relative errors w.r.t. the transformation parameter L for pricing the Bermudan geometric basket put option in dimension 2 with $L_I = 7$, $\beta = 2$, and $K = 50$. (c) The convergence of Bermudan prices to American price w.r.t. the number of time steps K for pricing the 2-d Bermudan geometric basket put option with $L_I = 8$, $\beta = 1$, and $L = 2$.

exercisable Bermudan option to approximate the American price. For the equidistant time step $\Delta t = T/K$, it is widely accepted that the Bermudan price approaches the American price as $\Delta t \to 0$ with a convergence rate $\mathcal{O}(\Delta t)$. For one single underlying

asset, this convergence rate was shown in [49] for the Black Scholes model. A similar convergence rate has been observed in [25] and [50] for Lévy models. In almost all pricing schemes based upon the dynamic programming, a more accurate price can be obtained with more exercise dates (but at a higher computational cost). One general approach to alleviate the cost but still guarantee the accuracy is to apply the Richardson extrapolation [51, 52]. Fig. 6c present the convergence of Bermudan price to American price as K increases using Algorithm 1.

6 Conclusions

In this work, we have developed a novel quadrature and sparse grid interpolation based algorithm for pricing American options with many underlying assets. Unlike most existing methods, it does not involve introducing artificial boundary data by avoiding truncating the computational domain, and that a significant reduction of the number of grid points by introducing a bubble function. The resulting multivariate function has been shown to have bounded mixed derivatives. Numerical experiments for American basket put options with the number of underlying assets up to 16 demonstrate excellent accuracy of the approach. Future work includes pricing max-call options for multiple underlying assets, which are benchmark test cases for high-dimensional American options. Max-call options pose computational challenges due to their unboundedness and thus require certain special treatment.

Acknowledgement

JY acknowledges support from the University of Hong Kong via the HKU Presidential PhD Scholar Programme (HKU-PS). The authors would like to thank the Isaac Newton Institute for Mathematical Sciences for support and hospitality during the programme Uncertainty Quantification and Stochastic Modelling of Materials when work on this paper was undertaken. This work was supported by EPSRC Grant Number EP/R014604/1. GL acknowledges the support from GRF (project number: 17317122) and Early Career Scheme (Project number: 27301921), RGC, Hong Kong. The authors thanks Prof. Michael Griebel (University of Bonn, Germany) for providing valuable literatures on option pricing and sparse grids.

References

[1] Zhang, G.: Exotic Options : a Guide to Second Generation Options, 2nd ed. edn. World Scientific, Singapore (1998)

[2] Andersen, L., Broadie, M.: Primal-dual simulation algorithm for pricing multidimensional american options. Management Science **50**(9), 1222–1234 (2004)

[3] Haugh, M., Kogan, L.: Pricing american options: a duality approach. Operations Research **52**(2), 258–270 (2004)

[4] Hu, W., Zastawniak, T.: Pricing high-dimensional american options by kernel ridge regression. Quantitative Finance **20**(5), 851–865 (2020)

[5] Kovalov, P., Linetsky, V., Marcozzi, M.: Pricing multi-asset american options: A finite element method-of-lines with smooth penalty. Journal of Scientific Computing **33**(3), 209–237 (2007)

[6] Nielsen, B., Skavhaug, O., Tveito, A.: Penalty methods for the numerical solution of american multi-asset option problems. Journal of Computational and Applied Mathematics **222**(1), 3–16 (2008)

[7] Reisinger, C., Wittum, G.: Efficient hierarchical approximation of high-dimensional option pricing problems. SIAM Journal on Scientific Computing **29**(1), 440–458 (2007)

[8] Scheidegger, S., Treccani, A.: Pricing american options under high-dimensional models with recursive adaptive sparse expectations. Journal of Financial Econometrics **19**(2), 258–290 (2021)

[9] Guyon, J., Henry-Labordère, P.: Nonlinear Option Pricing. Chapman & Hall/CRC financial mathematics series. CRC Press, Boca Raton (2014 - 2014)

[10] Merton, R.: Option pricing when underlying stock returns are discontinuous. Journal of financial economics **3**(1-2), 125–144 (1976)

[11] Bensoussan, A., Lions, J.: Applications of Variational Inequalities in Stochastic Control. Studies in mathematics and its applications ; v. 12. North-Holland Pub. Co., Amsterdam (1982)

[12] Jaillet, P., Lamberton, D., Lapeyre, B.: Variational inequalities and the pricing of american options. Acta Applicandae Mathematicae **21**(3), 263–289 (1990)

[13] McKean, H.: Appendix: A free boundary problem for the heat equation arising from a problem in mathematical economics. Industrial Management Review **6**(2), 32 (1965)

[14] Moerbeke, P.: Optimal stopping and free boundary problems. The Rocky Mountain Journal of Mathematics **4**(3), 539–578 (1974)

[15] Brennan, M., Schwartz, E.: The valuation of american put options. The Journal of Finance **32**(2), 449–462 (1977)

[16] Cox, J., Ross, S., Rubinstein, M.: Option pricing: A simplified approach. Journal of financial Economics **7**(3), 229–263 (1979)

[17] Amin, K., Khanna, A.: Convergence of american option values from discrete- to continuous-time financial models. Mathematical Finance **4**(4), 289–304 (1994)

[18] Boyle, P.: A lattice framework for option pricing with two state variables. Journal of financial and quantitative analysis **23**(1), 1–12 (1988)

[19] Bensoussan, A.: On the theory of option pricing. Acta Applicandae Mathematica **2**, 139–158 (1984)

[20] Achdou, Y., Pironneau, O.: Computational Methods for Option Pricing. Frontiers in applied mathematics. Society for Industrial and Applied Mathematics, Philadelphia (2005)

[21] Forsyth, P., Vetzal, K.: Quadratic convergence for valuing american options using a penalty method. SIAM Journal on Scientific Computing **23**(6), 2095–2122 (2002)

[22] Peskir, G., Shiryaev, A.: Optimal Stopping and Free-boundary Problems. Lectures in mathematics ETH Zürich. Birkhäuser Verlag, Basel (2006)

[23] Longstaff, F., Schwartz, E.: Valuing american options by simulation: a simple least-squares approach. The review of financial studies **14**(1), 113–147 (2001)

[24] Tsitsiklis, J., Van Roy, B.: Regression methods for pricing complex american-style options. IEEE Transactions on Neural Networks **12**(4), 694–703 (2001)

[25] Quecke, S.: Efficient numerical methods for pricing american options under lévy models. PhD thesis, Universität zu Köln (2007)

[26] Sullivan, M.: Valuing american put options using gaussian quadrature. The Review of Financial Studies **13**(1), 75–94 (2000)

[27] Glau, K., Mahlstedt, M., Potz, C.: A new approach for american option pricing: The dynamic chebyshev method. SIAM Journal on Scientific Computing **41**(1), 153–180 (2019)

[28] Bungartz, H.-J., Griebel, M.: Sparse grids. Acta numerica **13**, 147–269 (2004)

[29] Bayer, C., Ben Hammouda, C., Tempone, R.: Numerical smoothing with hierarchical adaptive sparse grids and quasi-monte carlo methods for efficient option pricing. Quantitative Finance, 1–19 (2021)

[30] Bungartz, H.-J., Dirnstorfer, S.: Multivariate quadrature on adaptive sparse grids. Computing **71**, 89–114 (2003)

[31] Holtz, M.: Sparse Grid Quadrature in High Dimensions with Applications in Finance and Insurance. Springer, Germany (2011)

[32] Bungartz, H.-J., Heinecke, A., Pflüger, D., Schraufstetter, S.: Option pricing with a direct adaptive sparse grid approach. Journal of Computational and Applied Mathematics **236**(15), 3741–3750 (2012)

[33] Barthelmann, V., Novak, E., Ritter, K.: High dimensional polynomial interpolation on sparse grids. Advances in Computational Mathematics **12**, 273–288 (2000)

[34] Boyd, J.: Chebyshev and Fourier Spectral Methods, 2nd ed., rev. edn. Dover Publications, Mineola, N.Y (2001)

[35] Zhu, Y.-L., Li, J.: Multi-factor financial derivatives on finite domains. Communications in Mathematical Sciences **1**(2), 343–359 (2003)

[36] Wasilkowski, G., Wozniakowski, H.: Explicit cost bounds of algorithms for multivariate tensor product problems. Journal of Complexity **11**(1), 1–56 (1995)

[37] Novak, E., Ritter, K.: Simple cubature formulas with high polynomial exactness. Constructive approximation **15**(4), 499–522 (1999)

[38] Kuo, F., Nuyens, D.: A practical guide to quasi-Monte Carlo methods. Tech. rep. KU Leuven (2016)

[39] Piazzola, C., Tamellini, L.: The Sparse Grids Matlab kit - a Matlab implementation of sparse grids for high-dimensional function approximation and uncertainty quantification. ArXiv (2203.09314) (2023)

[40] Adams, R., Fournier, J.: Sobolev Spaces, 2nd ed. edn. Pure and applied mathematics ; v. 140. Academic Press, Amsterdam (2003)

[41] Folland, G.: Real Analysis : Modern Techniques and Their Applications, 2nd ed. edn. Pure and applied mathematics. Wiley, New York (1999)

[42] Akhiezer, N.: Theory of Approximation. F. Ungar Pub. Co., New York (1956)

[43] Gerstner, T.: Sparse grid quadrature methods for computational finance. Habilitation, University of Bonn **77** (2007)

[44] Giles, M., Kuo, F., Sloan, I., Waterhouse, B.: Quasi-monte carlo for finance applications. ANZIAM Journal **50**, 308–323 (2008)

[45] Joy, C., Boyle, P., Tan, K.-S.: Quasi-monte carlo methods in numerical finance. Management science **42**(6), 926–938 (1996)

[46] L'Ecuyer, P.: Quasi-monte carlo methods with applications in finance. Finance and Stochastics **13**, 307–349 (2009)

[47] Griewank, A., Kuo, F., Leövey, H., Sloan, I.: High dimensional integration of kinks and jumps—smoothing by preintegration. Journal of Computational and Applied Mathematics **344**, 259–274 (2018)

[48] Liu, S., Owen, A.: Preintegration via active subspace. SIAM Journal on Numerical Analysis **61**(2), 495–514 (2023)

[49] Howison, S., Steinberg, M.: A matched asymptotic expansions approach to continuity corrections for discretely sampled options. part 1: Barrier options. Applied Mathematical Finance **14**(1), 63–89 (2007)

[50] Fang, F., Oosterlee, C.: Pricing early-exercise and discrete barrier options by fourier-cosine series expansions. Numerische Mathematik **114**(1), 27 (2009)

[51] Geske, R., Johnson, H.: The american put option valued analytically. The Journal of Finance **39**(5), 1511–1524 (1984)

[52] Chang, C.-C., Chung, S.-L., Stapleton, R.: Richardson extrapolation techniques for the pricing of american-style options. Journal of Futures Markets: Futures, Options, and Other Derivative Products **27**(8), 791–817 (2007)